

## Density functional band gaps of AlAs

H. Jin, G. L. Zhao, and D. Bagayoko\*

*Department of Physics, Southern University and A & M College, Baton Rouge, Louisiana 70813, USA*

(Received 13 February 2006; revised manuscript received 27 March 2006; published 27 June 2006)

We present results of *ab initio*, self-consistent calculations of electronic properties of AlAs in the zinc-blende structure. Our nonrelativistic calculations employed the generalized gradient approximation of density functional potential and Bagayoko, Zhao, and Williams implementation method of the linear combination of atomic orbitals formalism. Our calculated indirect band gaps at the  $X$  and  $L$  points are 2.15 and 2.38 eV, respectively, in good agreement with experimental values. The calculated direct gap at  $\Gamma$  is 25% smaller than the experimental one. We also present calculated total and partial densities of states and the electron effective mass at the bottom of the conduction band at  $\Gamma$ .

DOI: [10.1103/PhysRevB.73.245214](https://doi.org/10.1103/PhysRevB.73.245214)

PACS number(s): 71.15.Ap, 71.20.-b, 71.22.+i

### I. INTRODUCTION

AlAs has attracted much attention because it is not only one of the most important electronic and optoelectronic materials, but also a very essential component in GaAs-based heterostructures, superlattices, and quantum wells. There are numerous device applications of  $\text{Al}_x\text{Ga}_{1-x}\text{As}$  alloys, including diode lasers, light-emitting diodes, photodetectors, and electro-optic modulators. AlAs and its heterostructures have been studied extensively for both their scientific and technological relevance.<sup>1-7</sup>

The theoretical prediction of band structures, fundamental energy gaps, and effective masses of semiconductors and alloys is of great importance for the fabrication of the heterostructures and devices. Over the past 2 decades, there have been many theoretical calculations of the electronic structures of AlAs.<sup>3,5,7-19</sup> To our knowledge, however, except for the fitting approaches such as the tight-binding model,<sup>13,14,16</sup> almost all of the theoretical calculations of the band structure of AlAs led to band gaps that deviate from the experimental values<sup>3,7-12</sup> to varying degrees. Table I lists the referenced theoretical and experimental band gaps of AlAs. For the theoretical works, the table also shows the applicable potential and computational method. Unlike other III-V compounds, AlAs is an indirect band gap semiconductor with the conduction band minimum close to or at the  $X$  point<sup>7-12,19</sup> while the valence band maximum is at the gamma ( $\Gamma$ ) point. Usually, three band gaps are reported for the AlAs system: the minimum indirect band gap  $E_g^X$ , the direct gap  $E_g^\Gamma$ , and the second and larger indirect gap  $E_g^L$ . As can be seen from Table I, previous, *ab initio* local density approximation (LDA) calculations typically reported values of the minimum, indirect gap that are 36% to 47% off the measured one.<sup>4</sup> Although the agreement with experiment has been improved dramatically by using the Green function and screened Coulomb potential approximation and the pseudopotential method (GW-PP),<sup>15</sup> the Green function and screened Coulomb potential approximation and the quasiparticle approach (GW-QP),<sup>9</sup> and a semi-*ab initio* approach utilizing a minimum basis set of orthogonalized functions in a linear combination of atomic orbitals (OLCAO)<sup>8</sup> and an additional atomiclike potential, the discrepancies for the calculated band gaps  $E_g^X$ ,  $E_g^\Gamma$ , and  $E_g^L$  have remained significant. These band gaps, for the GW-PP<sup>15</sup>

and the GW-QP are 2.08, 2.75, and 2.79 eV for the former and 2.09, 3.26, and 2.81 for the latter. While the improvement for the minimum, indirect gap is significant, the overestimations of the larger, indirect gap are by 18% and 28% for the GW-PP and GW-QP calculations, respectively.

The above discrepancies are key motivations for this work that employs a GGA potential and the Bagayoko, Zhao and Williams (BZW) method<sup>20,21</sup> within the linear combination of atomic orbital formalism (LCAO). The BZW method has been successfully applied to reproduce or to predict the band gaps of numerous semiconductors, including cubic InN,<sup>22</sup> wurtzite InN,<sup>23</sup> GaN, Si, and C,<sup>21</sup> and carbon nanotubes.<sup>24,25</sup>

### II. COMPUTATIONAL METHOD AND DETAILS

Our nonrelativistic calculations employed a nonlocal density functional potential from the generalized gradient approximation (GGA).<sup>26-28</sup> We utilized the formalism of the linear combination of atomic orbitals (LCAO) in real space. The implementation of the BZW method in carrying out the self-consistent computations is the major, distinctive feature of the present work as compared to previous works on AlAs. The details of the BZW procedure are widely available in the literature<sup>21-25</sup> and are discussed further below. A brief overview of its implementation follows.

In the implementation of the BZW procedure, we started the self-consistent calculations with a minimal basis set, i.e., the basis set just accounting for all the electrons in the atomic or ionic species present in the system under study. For AlAs, we chose the ions  $\text{Al}^{1+}$  and  $\text{As}^{1-}$  for our self-consistent calculations, as preliminary studies indicated charge transfers closer to these species, i.e., the self-consistent system is approximately  $\text{Al}^{0.94+}\text{As}^{0.94-}$ . We subsequently carried out several other self-consistent calculations with larger and larger basis sets by augmenting with one or more ionic orbitals that belong to the next and lowest-lying energy levels in  $\text{Al}^{1+}$  or  $\text{As}^{1-}$ . The occupied bands of a given calculation are compared to those of the previous one until they are found to be identical in numerical values, curvature, and branching, within computational uncertainties. The results reported here are those of the calculation before the last one. The basis set for this calculation (i.e., VII for AlAs) is referred to as the optimal basis set. As explained further be-

TABLE I. Comparison of theoretical and experimental band gaps of zinc-blende AIAs. The three band gaps at respective  $\Gamma_{15v}-X_{1c}$ ,  $\Gamma_{15v}-\Gamma_{1c}$ , and  $\Gamma_{15v}-L_{1c}$ .

Potential	Computational method	$E_g^X$ (eV)	$E_g^\Gamma$ (eV)	$E_g^L$ (eV)
Experiment 1	Photoluminescence ( $T=12$ K)	2.25 <sup>a</sup>		
Experiment 2	Excitonic gap, photoluminescence ( $T=4$ K)	2.23 <sup>b</sup>	3.13 <sup>b</sup>	
	Excitonic gap, photoluminescence ( $T=300$ K)	2.15 <sup>b</sup>	3.03 <sup>b</sup>	
Experiment 3	Transport ( $T=295$ K)	2.16 <sup>c</sup>	2.98 <sup>c</sup>	2.36 <sup>c</sup>
GGA	LCAO-BZW (Present work) $a=5.66$ Å	2.15	2.35	2.38
GGA	LCAO-BZW (Present work) $a=5.6524$ Å	2.14	2.38	2.39
LDA	Projector-augmented-wave (PAW)	1.32 <sup>d</sup>	1.94 <sup>d</sup>	2.06 <sup>d</sup>
GW	PAW	1.57 <sup>d</sup>	2.7 <sup>d</sup>	2.73 <sup>d</sup>
LDA	Pseudopotential method (PP)	1.20 <sup>e</sup>	1.77 <sup>e</sup>	1.89 <sup>e</sup>
GW	PP	2.08 <sup>e</sup>	2.75 <sup>e</sup>	2.79 <sup>e</sup>
LDA	<i>Ab initio</i> PP	1.44 <sup>f</sup>	2.35 <sup>f</sup>	2.12 <sup>f</sup>
LDF	First-principles full-potential self-consistent linearized-muffin-tin-orbital (LMTO)	1.31 <sup>g</sup>		
	Ab-initio PP	1.3 <sup>h</sup>	2.5 <sup>h</sup>	
LDA	Self-consistent full-potential linearized-augmented-plane-wave (FLAPW)	1.36 <sup>i</sup>	1.95 <sup>i</sup>	2.07 <sup>i</sup>
GW	Quasiparticle (QP)	2.09 <sup>j</sup>	3.26 <sup>j</sup>	3.03 <sup>j</sup>
LDF	Minimal basis semi- <i>ab initio</i> orthogonalized LCAO method	2.37 <sup>k</sup>	2.79 <sup>k</sup>	2.81 <sup>k</sup>
Tight-binding model (TBM)	PP	2.21 <sup>l</sup>	2.79 <sup>l</sup>	2.48 <sup>l</sup>
TBM		2.142 <sup>m</sup>	2.998 <sup>m</sup>	2.313 <sup>m</sup>
TBM		2.262 <sup>n</sup>	2.974 <sup>n</sup>	2.756 <sup>n</sup>

<sup>a</sup>Reference4.<sup>b</sup>Reference1.<sup>c</sup>Reference2.<sup>d</sup>Reference7.<sup>e</sup>Reference15.<sup>f</sup>Reference12.<sup>g</sup>Reference11.<sup>h</sup>Reference10.<sup>i</sup>Reference3.<sup>j</sup>Reference9.<sup>k</sup>Reference8.<sup>l</sup>Reference16.<sup>m</sup>Reference13.<sup>n</sup>Reference14.

low in the discussion section, upon the convergence of the charge density, potential, and occupied energy levels, as is the case for the calculation with the optimal basis set, computations with larger basis set are inherently affected by a basis set and variational effect. This effect stems from the use of a variational approach where the charge density is computed using only the wave functions of occupied states and consequences of the Rayleigh theorem.<sup>21-23</sup> Table II shows the basis sets employed in the various, self-consistent calculations we performed for AIAs. The results discussed here are those from Calculation VII for which the basis set is optimal in the sense specified above.

We utilized an expanded version of the electronic structure calculation program package from the Ames Laboratory of the Department of Energy (DOE).<sup>29-31</sup> AIAs, in the zinc-blende structure, is a member of the III-V family and belongs to the  $T_d^2-F\bar{4}3m$  space group. As per Table I, only Experiment 3, done at a temperature of 295 K, provides<sup>2</sup> values for the two indirect and one direct gaps noted above. For comparison purposes, we selected the experimental lattice parameter of  $a=5.66$  Å for a temperature of 291 K.<sup>34</sup> Except for

the gap values shown in Table I for a zero-temperature lattice constant<sup>6</sup> of 5.6524 Å, the results discussed here are for the above room temperature lattice constant. The atomic wave

TABLE II. The atomic orbitals used in calculations I to VIII for AIAs. Superscript zeros indicate added orbitals representing unoccupied atomic states.

Basis set 0: core-state orbitals in calculations I to VIII: Al (1s), As (1s,2s,2p)
Basis set I: Al(1s,2s,2p,3s), As(1s,2s,2p,3s,3p,3d,4s,4p)
Basis set II: Set I plus Al(3p <sup>0</sup> )
Basis set III: Set II plus As(5s <sup>0</sup> )
Basis set IV: Set III plus Al(4s <sup>0</sup> )
Basis set V: Set IV plus As(4d <sup>0</sup> )
Basis set VI: Set V plus Al(3d <sup>0</sup> )
Basis set VII: Set VI plus As(5p <sup>0</sup> )
Basis set VIII: Set VII plus Al(4p <sup>0</sup> )

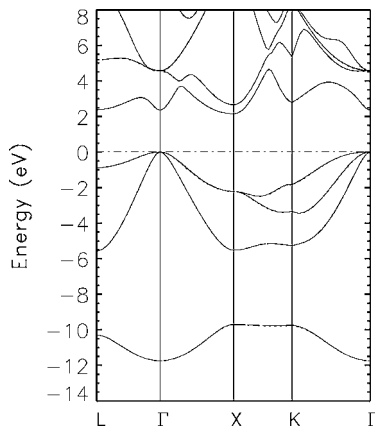


FIG. 1. Electronic band structure of AIAs. The solid lines represent the results from Calculation VII and the dashed lines those from Calculation VIII. Other results in Tables I and III and Figs. 2 and 3 are from Calculation VII. The lattice constant is 5.66 Å.

functions of the ionic states of  $\text{Al}^{1+}$  and  $\text{As}^{1-}$  were obtained from self-consistent, *ab initio*, atomic calculations. The radial parts of the atomic wave functions were expanded in terms of Gaussian functions. Sets of even-tempered Gaussian exponentials were employed with a minimum of 0.10 for both Al and As, and a maximum of  $4.5000 \times 10^4$  for Al and  $1.5000 \times 10^5$  for As, in atomic units. We used 19, 19, and 17 orbitals for the s, p, and d states for both Al and As. A mesh of 60 k points, with proper weights in the irreducible Brillouin zone, was employed in the self-consistent iterations. The computational error for the valence charge was about 0.000129 for 34 electrons. The self-consistent potentials converged to a difference of  $10^{-5}$  after about 30 iterations. The total number of iterations varied with the input potentials. The basis sets for each of the self-consistent calculations used in the BZW procedure in this work are listed in Table II. The optimal basis set for the AIAs calculation is the basis set for calculation VII.

### III. RESULTS

Figure 1 shows the band structure of AIAs at high symmetry points and along high symmetry lines in the Brillouin zone. The calculated conduction band minimum is at the X point while the valence band maximum is at  $\Gamma$ , in agreement with experiment. The energy levels at high symmetry points

TABLE III. Electronic energies (eV) at high symmetry points, with the top of the valence band set to 0 eV. Data are from Calculation VII for a lattice constant of 5.66 Å.

$\Gamma$	X	L	K
-11.74	-9.70	-10.30	-9.74
0.00	-5.52	-5.56	-5.27
0.00	-2.21	-0.88	-3.33
2.35	2.15	2.38	-1.84
4.58	2.65	5.20	2.79

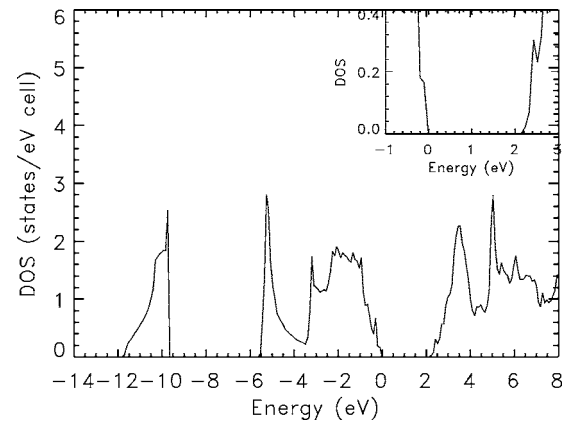


FIG. 2. The calculated density of states for AIAs, as obtained from the bands from Calculation VII, for a lattice constant of 5.66 Å. The inset shows the practically measurable band gap from 2.14 to 2.4 eV.

in the Brillouin zone are listed in Table III. Our calculated, indirect, fundamental band gap value of 2.15 eV agrees very well with the experimental values of 2.15 and 2.16 eV, at room temperature, and is lower, by less than 5%, than the zero temperature values of 2.23 and 2.25 eV, as shown in Table I. Similarly, the calculated indirect band gap at the L point, 2.38 eV, agrees very well with the experimental finding of 2.36 eV. However, our direct band gap of 2.35 eV is about 21% and 25% lower than the measured values, as discussed further below.

Figures 2 and 3 show the total (DOS) and partial densities of states (PDOS) for AIAs, respectively, as obtained from Calculation VII. The total DOS curves, particularly the inset, show that the practically measurable band gap could be anywhere between 2.14 and 2.4 eV, where the latter corresponds to a value of 0.1 for the DOS, in excellent agreement with experiments.<sup>1,2,5</sup> The lowest peak between -11.8 and -9.7 eV arises from the Al(3p) and As(4s) orbitals. The peaks appearing between -5.6 and 0 eV stem from Al(3s), Al(3p), and As(4p) orbitals. A significant hybridization of

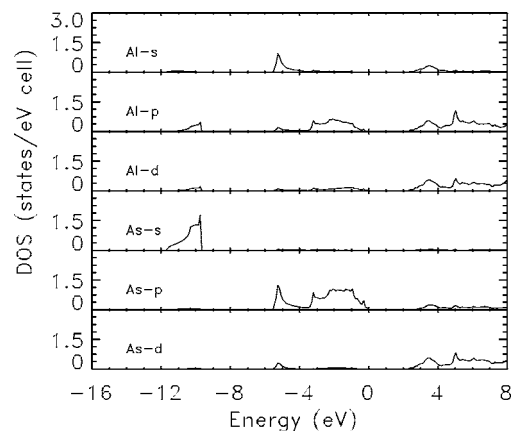


FIG. 3. The partial density of states (PDOS) for AIAs from the contribution of the s, p, and d states of Al and As atoms, respectively. These PDOS are derived from the bands from Calculation VII, for a lattice constant of 5.66 Å.

Al(4*p*), Al(3*d*), and As(4*d*) orbitals is apparent in the PDOS curve in Fig. 3.

Our calculated electron effective mass of AlAs,  $m^*$ , at the bottom of the conduction band at the  $\Gamma$  point, is  $0.15 m_0$ , where  $m_0$  is the free-electron mass. This result is also in excellent agreement with the experimental value of  $0.15 m_0$  in Ref. 32 and is 21% higher than the  $0.124 m_0$  estimated from a fit to absorption data.<sup>33</sup>

#### IV. DISCUSSIONS

In comparison to previous density functional and other calculations, this work has resolved most of the discrepancies between experiment and theory. Previous density functional calculations, as per the content of Table I, woefully underestimated the indirect band gaps and the direct one. The GW calculations improved the agreement between theory and experiment for the fundamental, indirect gap, by reducing the underestimation to about 3% from the room temperature value. For the larger indirect gap at *L*, however, they overestimated significantly (by 18% and 28%). While GW-PP<sup>15</sup> underestimates the room temperature direct gap by close to 8%, the GW-QP<sup>9</sup> overestimates it by 9%. Vurgaftman *et al.*<sup>6</sup> underscored the difficulties associated with the experimental determination of the direct gap at  $\Gamma$ . These difficulties are apparent in the work of Monemar<sup>1</sup> where high impurity concentrations caused a broadening of exciton spectra. Consequently, the well-defined dip in the spectrum, that would have indicated the direct gap, is replaced by a much broader dip from the uncertain location of which one extracts the value of the direct gap. We expect the uncertainties associated with the determination of this direct gap to contribute to the unusual deviation of our calculated value from experiment. Further, given that this gap is not the minimum one, GGA-BZW calculations are not necessarily expected to describe it correctly from a ground state theory as it does for the fundamental band gap.<sup>20–25</sup>

A central issue in these discussions relates to the physical and mathematical reasons that explain the success of the BZW method where many others have failed, including some rather sophisticated approaches that go beyond density functional theory. The answer resides in a thorough understanding of basis set related effects on the outcomes of these calculations. Specifically, as discussed by Bagayoko *et al.*,<sup>35</sup> LCAO type calculations have to ascertain the completeness of the basis set. In doing so, one typically includes diffuse orbitals, with relatively small exponents, to accommodate the charge redistribution in the molecular or solid state environments as compared to those for atoms or ions. Additionally, one has to provide for angular symmetries that may arise in molecular or solid environments. Most works cited herein appear to have handled these two points correctly.

There is still a nontrivial basis set related effect distinct from the issues of angular symmetry and of diffuse orbitals. The preoccupation for guaranteeing the completeness of the basis set explains the use of as large basis sets as possible, as long as linear dependency is avoided. Consequently, no particular limit is placed on the size of the basis set. This size often varies widely from one group of investigators to an-

other, even for the same system and for similar orbitals (i.e., Gaussians). The Rayleigh theorem,<sup>36,37</sup> however, indicates that serious problems could be associated with arbitrarily large basis sets. The statement of this rigorous, mathematical theorem follows: *Let an eigenvalue equation be solved twice, by an LCAO method, respectively, with  $N$  and  $(N+1)$  orbitals—such that the  $(N+1)$  orbitals of Calculation II include all the  $N$  orbitals of Calculation I plus an additional one—and let the eigenvalues from the two calculations be ordered from the lowest ( $\epsilon_1^N$  and  $\epsilon_1^{(N+1)}$  for I and II, respectively) to the highest ( $\epsilon_N^N$  and  $\epsilon_{(N+1)}^{(N+1)}$ , respectively), then the theorem states that  $\epsilon_i^{(N+1)} \leq \epsilon_i^N$  for all  $i \leq N$ .* Alternatively, this theorem states that a variational eigenvalue, upon an increase of the basis set (and hence of the dimension of the matrix), is not increased. It either stays the same (if it is equal to the exact, physical eigenvalue of the matrix) or it decreases to approach this exact eigenvalue from above. This theorem therefore points to the need to utilize as large a basis set as possible in order to lower variational eigenvalues to reach the exact ones. Such a large basis set is also needed to ensure completeness. Bagayoko, Zhao, and Williams<sup>20,21</sup> identified a basis set and variational effect stemming from any lowering of unoccupied energy levels or bands, for molecules or solids, respectively, when the occupied levels or bands have converged (vis-à-vis an increase of the basis set). The effect can exist in any variational calculations for which the occupied and unoccupied states are not treated in identical manners. Specifically, for all variational calculations of which we know, the occupied and unoccupied states are treated in fundamentally different manners: in the iterative process toward self-consistency, the charge density is constructed or reconstructed *using only the wave functions of the occupied states*. Hence, only the wave functions of these states affect the charge density, the potential, and the Hamiltonian itself, i.e., the physics of the system. It is therefore necessary to guarantee that an applicable basis set is large enough to ensure the convergence of the occupied levels or bands vis-à-vis the size of the basis set. To do so, Bagayoko, Zhao, and Williams (BZW) introduced their method that requires the utilization of a minimum basis set for the first, self-consistent calculation. The outcomes of this first calculation are generally not the correct solutions for the physical system under study. The method therefore requires subsequent calculations where the basis set is methodically augmented as described above and elsewhere.<sup>20,21</sup> The *occupied* energy levels or bands of a calculation are compared to those of the previous one that has a smaller basis set. This process continues until calculation  $N$  and  $(N+1)$  have the same occupied energy levels or bands, within applicable uncertainties. We then select the outputs of calculation  $N$  as the physical description of the system. Indeed, in light of the Rayleigh theorem, some unoccupied energy levels or bands of Calculation  $(N+1)$  are generally lower as compared to their counterpart from Calculation  $N$ . The BZW method ascribes any such additional lowering of an unoccupied band, while the occupied ones do not change, to mathematical artifacts stemming directly from the Rayleigh theorem. While the method applies to all variational calculations of the Rayleigh-Ritz type that employ an LCAO approach, it is particularly perti-

ment for density functional calculations. Indeed, density functional theory is fundamentally a ground state theory. The BZW method verifiably guarantees the proper description of the ground state with a basis that is sufficiently large. Variational calculations that do not employ the method generally have large enough basis sets to describe the applicable system. However, they do not actually verify that the size of the basis set converged vis-à-vis the description of the occupied states and they do not avoid Rayleigh-theorem related lowering of some unoccupied levels or bands on purely mathematical ground—given that the Hamiltonian (i.e., the physics) does not change once the optimal basis size of the BZW method is attained.

## V. CONCLUSION

In conclusion, we successfully performed *ab initio*, self-consistent GGA-BZW calculations for the band structure of a

zinc-blende AIAs semiconductor. Our calculated band gaps, except for the direct gap at  $\Gamma$ , are in excellent agreement with measured values. Our calculated effective mass also agrees very well with a directly determined experimental value and disagrees with an estimate derived from fitting to absorption data.

## ACKNOWLEDGMENTS

This work was funded in part by the Department of the Navy, Office of Naval Research (ONR, Grant No. N00014-05-1-0009), NASA (Award Nos. NCC 2-1344 and NAG 5-10253), and by the National Science Foundation (Award No. HRD 0000272). The authors are indebted to S. Hasan for his excellent technical support with the computing facilities.

---

\*Corresponding author. Email address: bagayoko@phys.subr.edu or babayoko@aol.com

<sup>1</sup>B. Monemar, Phys. Rev. B **8**, 5711 (1973).

<sup>2</sup>H. J. Lee, L. Y. Juravel, J. C. Woolley, and A. J. Spring Thorpe, Phys. Rev. B **21**, 659 (1980).

<sup>3</sup>B. I. Min, S. Massidda, and A. J. Freeman, Phys. Rev. B **38**, 1970 (1988).

<sup>4</sup>M. Guzzi, E. Grilli, S. Oggioni, J. L. Staehli, C. Bosio, and L. Pavesi, Phys. Rev. B **45**, 10951 (1992).

<sup>5</sup>Ming-Zhu Huang and W. Y. Ching, Phys. Rev. B **47**, 9449 (1993).

<sup>6</sup>I. Vurgaftman, J. R. Meyer, and L. R. Ram-Mohan, J. Appl. Phys. **89**, 5815 (2001).

<sup>7</sup>S. Lebegue, B. Arnaud, M. Alouani, and P. E. Bloechl, Phys. Rev. B **67**, 155208 (2003).

<sup>8</sup>Ming-Zhu Huang and W. Y. Ching, J. Phys. Chem. Solids **46**, 977 (1985).

<sup>9</sup>R. W. Godby, M. Schluter, and L. J. Sham, Phys. Rev. B **35**, 4170 (1987).

<sup>10</sup>P. Boguslawski and I. Gorczyca, Acta Phys. Pol. A **80**, 433 (1991).

<sup>11</sup>Bal K. Agrawal and Savitri Agrawal, Phys. Rev. B **45**, 8321 (1992).

<sup>12</sup>Q. Guo, C. K. Ong, H. C. Poon, and Y. P. Feng, Phys. Status Solidi B **197**, 111 (1996).

<sup>13</sup>Timothy B. Boykin, Phys. Rev. B **54**, 8107 (1996).

<sup>14</sup>J. P. Loehr and D. N. Talwar, Phys. Rev. B **55**, 4353 (1997).

<sup>15</sup>E. L. Shirley, X. Zhu, and S. G. Louie, Phys. Rev. B **56**, 6648 (1997).

<sup>16</sup>An-Ban Chen and Arden Sher, Phys. Rev. B **22**, 3886 (1980).

<sup>17</sup>K. A. Mader and A. Zunger, Phys. Rev. B **50**, 17393 (1994).

<sup>18</sup>E. Hess, I. Topol, K.-R. Schulze, H. Neumann, and K. Unger, Phys. Status Solidi B **55**, 187 (1973).

<sup>19</sup>J. J. Finley, R. J. Teissier, M. S. Skolnick, J. W. Cockburn, G. A.

Roberts, R. Grey, G. Hill, M. A. Pate, and R. Planel, Phys. Rev. B **58**, 10619 (1998).

<sup>20</sup>D. Bagayoko, G. L. Zhao, J. D. Fan, and J. T. Wang, J. Phys.: Condens. Matter **10**, 5645 (1998).

<sup>21</sup>G. L. Zhao, D. Bagayoko, and T. D. Williams, Phys. Rev. B **60**, 1563 (1999).

<sup>22</sup>D. Bagayoko, L. Franklin, and G. L. Zhao, J. Appl. Phys. **96**, 4297 (2004).

<sup>23</sup>D. Bagayoko and L. Franklin, J. Appl. Phys. **97**, 123708 (2005).

<sup>24</sup>A. Pullen, G. L. Zhao, D. Bagayoko, and L. Yang, Phys. Rev. B **71**, 205410 (2005).

<sup>25</sup>G. L. Zhao, D. Bagayoko, and L. Yang, Phys. Rev. B **69**, 245416 (2004).

<sup>26</sup>J. P. Perdew, K. Burke, and Y. Wang, Phys. Rev. B **54**, 16533 (1996); see also Phys. Rev. B **57**, 14999 (1998).

<sup>27</sup>J. P. Perdew and Y. Wang, Phys. Rev. B **33**, 8800 (1986).

<sup>28</sup>J. P. Perdew, Phys. Rev. B **33**, 8822 (1986).

<sup>29</sup>P. J. Feibelman, J. A. Appelbaum, and D. R. Hamann, Phys. Rev. B **20**, 1433 (1979).

<sup>30</sup>B. N. Harmon, W. Weber, and D. R. Hamann, Phys. Rev. B **25**, 1109 (1982).

<sup>31</sup>G. L. Zhao, T. C. Leung, B. N. Harmon, M. Keil, M. Mullner, and W. Weber, Phys. Rev. B **40**, 7999 (1989).

<sup>32</sup>M. Zachau, F. Koch, G. Weimann, and W. Schlapp, Phys. Rev. B **33**, 8564 (1986).

<sup>33</sup>W. P. Dumke, M. R. Lorenz, and G. D. Pettit, Phys. Rev. B **5**, 2978 (1972).

<sup>34</sup>W. B. Pearson, *A Handbook of Lattice Spacing and Structure of Metals and Alloys* (Pergamon Press, Oxford-London, 1967).

<sup>35</sup>D. Bagayoko and Pui-Man Lam at SUBR; Nathan Brener and Joseph Callaway at LSU; Phys. Rev. B **54**, 12184 (1996).

<sup>36</sup>D. Bagayoko, Int. J. Quantum Chem. **17**, 527 (1983).

<sup>37</sup>S. H. Gould, *Variational Methods for Eigenvalue Problems* (University of Toronto Press, Toronto, 1957), Chap. 2.